Spectrochimica Acta Part A: Molecular and Biomolecular Spectroscopy 275 (2022) 121135

Contents lists available at ScienceDirect

Spectrochimica Acta Part A: Molecular and Biomolecular Spectroscopy

journal homepage: www.elsevier.com/locate/saa

High resolution FTIR spectroscopy of germane: First study of $^{76}GeH_4$ in the region of Tetrad of the strongly interacting $\nu_1 + \nu_2, \nu_1 + \nu_4, \nu_2 + \nu_3$ and $\nu_3 + \nu_4$ ro–vibrational bands

O.N. Ulenikov [a,*], O.V. Gromova [a], E.S. Bekhtereva [a], N.I. Nikolaeva [a], I.A. Velmuzhova [b], M.A. Koshelev [c]

[a] Research School of High–Energy Physics, National Research Tomsk Polytechnic University, Tomsk 634050, Russia
[b] G.G. Devyatykh Institute of Chemistry of High Purity Substances, Russian Academy of Sciences, Nizhny Novgorod 603950, Russia
[c] Institute of Applied Physics, Russian Academy of Sciences, 603950 Nizhny Novgorod, Russia

HIGHLIGHTS

- The $\nu1 + \nu2/\nu1 + \nu4/\nu2 + \nu3/\nu3 + \nu4$ strongly interacting bands of GeH_4.
- Resonance interactions in spherical top molecules.
- Determination of spectroscopic parameters.

GRAPHICAL ABSTRACT

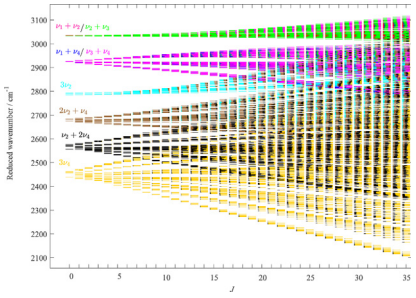

ARTICLE INFO

Article history:
Received 19 December 2021
Received in revised form 15 February 2022
Accepted 8 March 2022
Available online 12 March 2022

Keywords:
The $\nu_1 + \nu_2, \nu_1 + \nu_4, \nu_2 + \nu_3$ and $\nu_3 + \nu_4$ strongly interacting bands of GeH4
Resonance interactions in spherical top molecules
Determination of spectroscopic parameters

ABSTRACT

The infrared spectra of germane, purified and enriched up to 88.1% of $^{76}GeH_4$, was measured at the temperature of (22.6 ± 0.1) °C and different pressures with a Bruker Fourier transform infrared spectrometer IFS125HR and analyzed for the first time in the region of 2700–3200 cm^{-1} where the stretching–bending Tetrad ($\nu_1 + \nu_2, \nu_1 + \nu_4, \nu_2 + \nu_3$ and $\nu_3 + \nu_4$ bands) of the ro–vibrational Octad of germane is located. The 3595 transitions belonging to the eight sub–bands of the Tetrad were assigned and theoretically analysed in the frame of the effective Hamiltonian model. The obtained set of 106 fitted parameters reproduces the initial 3595 experimental line positions with the $d_{rms} = 6.81 \times 10^{-4}$ cm^{-1}. The presence of numerous resonance interactions in the Tetrad is discussed.

1. Introduction

The knowledge of spectroscopic characteristics of different isotopologues of GeH_4 is important in many fields of science and technology, e.g., for the production of high purity single–crystal germanium which can be used simultaneously as source of a double beta decay of its nuclei and as a detector of such processes (see, e.g., Refs. [1,2]), in astrophysics and planetology (studying the atmospheres of giant gas–planets, such as Jupiter and Saturn, see, e.g., [3–11]), in physical chemistry (germane, as well as, silane and methane, [12,13], can be considered as prototype of numerous organic molecules), etc. One of the important problems of chemical physics is the precise determination of intramolecular multidimensional potential and dipole moment surfaces, which can be used in numerous applied investigations. This problem can be solved by semi–empirical methods, [14], or on the basis of the *ab initio* calculations (see, e.g., [15]). In both cases, knowledge of

* Corresponding author.
E-mail address: Ulenikov@mail.ru (O.N. Ulenikov).

https://doi.org/10.1016/j.saa.2022.121135
1386-1425/

high accurate spectroscopic information not only on the main species, but also on all possible isotopologues is very important. To summarize, the high accurate spectroscopic information about characteristics of spectral lines (both line positions and line strengths) of different isotopologues of the germane molecule is very important and, as a consequence, for many years the germane molecule has been extensively studied in spectroscopy (see [16–62] and references therein).

Germane in a natural isotopic composition produces complex infrared spectra, not least as five stable isotopologues exist in proper abundances with mass numbers 70 (20.55%), 72 (27.37%), 73 (7.67%), 74 (36.74%), and 76 (7.67%). Additional complexity of the germane spectra arises from the presence of strongly interacting pairs of its fundamentals, ν_2/ν_4 and ν_1/ν_3. Germane is a spherical top molecule. It (1). has no permanent dipole moment, and (2). particularities of the $k-l$-splittings in such molecules lead to the appearance of only one strong transition in any component of the $k-l$ triplet (all other transitions are considerably weaker), see, e.g., [63,64]. As a consequence, the usability of the Ground State Combination Differences method which is efficient in the study of molecules of different type (see, *e.g.*, Refs. [65–71]) is very limited as applied to germane, and the assignment of transitions in infrared spectra of this molecule is not a simple problem.

In the present work we focus on the study of the $\nu_1+\nu_2, \nu_1+\nu_4, \nu_2+\nu_3$ and $\nu_3+\nu_4$ stretching–bending Tetrad of the $^{76}GeH_4$ specially enriched species which, to our knowledge, was not analysed before. The use of enriched sample made it possible for us to significantly reduce difficulties in the spectrum analyzing connecting with the need to take into account the presence of other germane isotopologues in the spectrum.

2. Experimental

The high–resolution spectra of germane were observed using a Bruker IFS125HR Fourier transform spectrometer. The experimental details are presented in Table 1.

The gas sample of germane contained $^{76}GeH_4$ (88.1%), $^{76}GeH_4$ (11.5%), $^{73}GeH_4$ (0.07%), $^{72}GeH_4$ (0.17%), and $^{70}GeH_4$ (0.12%) isotopologues. It was obtained in the following way. First, the sample of germane in natural abundance was synthesized at the Institute of Chemistry of High–Purity Substances of the Russian Academy of Sciences by a reaction between germanium tetrachloride and sodium borohydride with subsequent purification by the rectification method. Then the sample was enriched with the ^{76}Ge isotope using the centrifugal method at the Joint Stock Company "Production Association Electrochemical Plant", Zelenogorsk, Russia. The enriched sample was repeatedly purified by the rectification method. Analysis of the sample impurities was carried out by methods of gas chromatography, gas chromatography/mass spectrometry and high resolution FTIR spectroscopy, [72]. The content of hydrocarbon, carbon dioxide, di–, and tri–germane impurities in the enriched sample was less than 10^{-5} mol%, 10^{-4} mol% and $10^{-1}-10^{-3}$ mol%, respectively. The amount of the other impurities was less than 3×10^{-5} mol%.

The spectra were recorded in the frequency range 1800–4500 cm^{-1} using a Globar source, a liquid nitrogen cooled indium antimonide (InSb) detector and a KBr beam splitter. The resolution due to the maximum optical path difference was 0.003 cm^{-1}. A multi–pass White cell with a 0.375 m base path length was used with significantly different number of passes. The cell was permanently connected to the vacuum system with a gas sample system, a turbo–molecular pump station, and capacitance pressure gauges covering the 10^{-3}–100 Torr range. The optical compartment of the spectrometer was evacuated by a mechanical pump down to 0.02 Torr (or less) and that pressure remained during the experiment.

The final spectra (Fig. 1) were produced by the co–addition of about 1000 scans and processed with Norton–Beer (weak) apodization function using a zero–filling factor of 2. In total, three spectra were recorded at two different optical path lengths (0.75 and 3.75 m) and three different pressures, 0.3, 1.5 and 3 Torr (spectrum I, II and III, respectively), to cover a wider range of J numbers. The wavenumber scale of the spectrometer was calibrated by use of most intense and well resolved H_2O and CO_2 reference lines, showed up in all spectra, and HITRAN (2016) line list [73]. After calibration the standard deviation of the difference between the measured and tabulated peak positions was estimated to be about 2×10^{-4} cm^{-1}. Comparison of the positions of unsaturated unblended lines in different experimental spectra shown their agreement within $\pm10^{-4}$ cm^{-1}, which demonstrates a negligible effect of the pressure shifting and good data precision.

3. Brief theoretical background

Because of the symmetry of the GeH_4 molecule, its nine vibrational coordinates are distributed between four vibrational modes: one nondegenerate (q_1, A_1), one doubly degenerate (q_2, E), and two triply degenerate (q_3 and q_4, F_2). It is well known (see, e.g., [74–76]) that ro–vibrational states of such molecules are divided into groups (polyads) of more or less isolated states which interact with each other inside of the polyad. In general, for the $^{M}X^{m}Y_4$ (T_d symmetry) molecule (because of the approximate relationship of harmonic frequencies $\omega_1\simeq\omega_3\simeq2\omega_2\simeq2\omega_4$) both the fundamental and overtone and vibrational combination levels are grouped into so–called polyads of interacting vibrational levels of similar energy. These polyads usually characterized by symbol P_n ($n=2\nu_1+\nu_2+2\nu_3+\nu_4$; n is called as "polyad quantum number"), where ν_1, ν_2, ν_3 and ν_4, are quantum numbers of vibrational levels (in this case, each vibrational level can consist of several sub–levels of different symmetry; the polyad nomenclature is shown in Table 2). It is necessary to note that, with increasing of the mass of the $^{M}X^{m}Y_4$ molecule, differences between ω_1 and ω_3 and between ω_2 and ω_4 are decreased and, at the same time, relative values $|\omega_3-\omega_4|/|\omega_2-\omega_4|$ and $|\omega_3-\omega_4|/|\omega_3-\omega_1|$ are increased. As a consequence, each polyad is divided into separate sub–polyads which levels strongly interact with each other but only slightly interact with levels of other sub–polyads. In accordance with the above said, the Octad polyad, which is discussed in this paper, can be deviled into two Tetrads (four bending levels, $3\nu_2, 2\nu_2+\nu_4, \nu_2+2\nu_4, 3\nu_4$, which consists of 16 sub–levels; and

Table 1
Experimental setup for the regions 1800–4500 cm^{-1} of the infrared spectrum of $^{M}GeH_4$ ($M=76,74$).

Spectr.	Resolution /cm^{-1}	Measuring time/h	No. of scans	Source	Detector	Beam-splitter	Opt. path-length/m	Aperture /mm	Temp. /°C	Pressure /Torr	Calibr. gas
I	0.003	40.2	1200	Globar	InSb	KBr	3.75	1.0	22.7	0.3	H_2O, CO_2
II	0.003	36.9	1100	Globar	InSb	KBr	0.75	1.0	28.8	1.5	H_2O, CO_2
III	0.003	35.2	1050	Globar	InSb	KBr	3.75	1.0	22.6	3.0	H_2O, CO_2

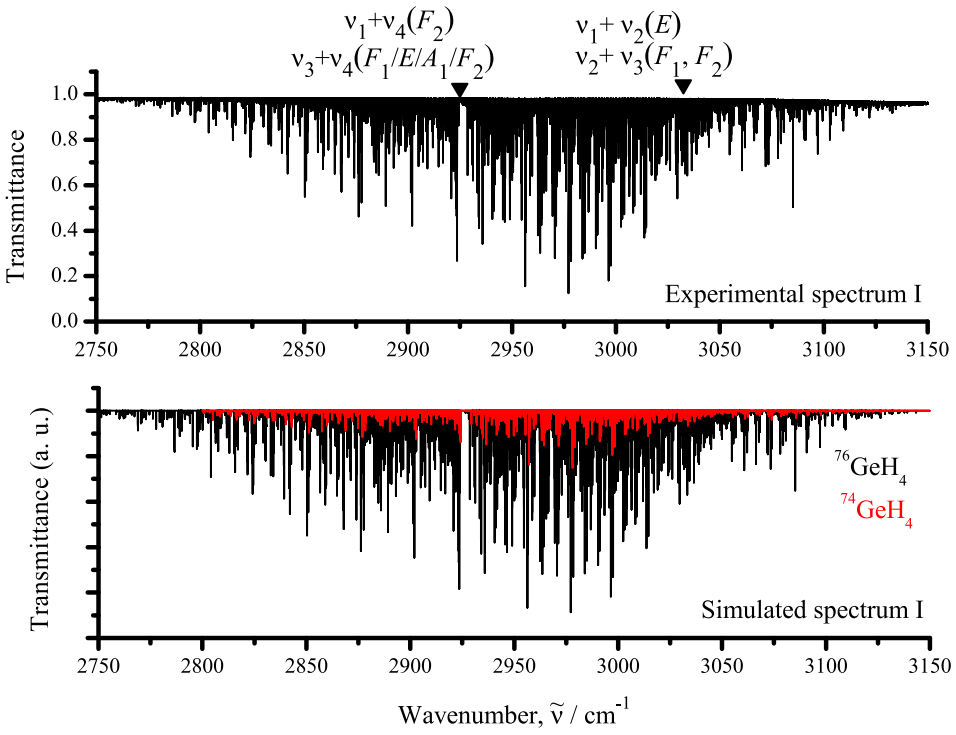

Fig. 1. Survey spectrum (upper trace) of GeH_4 in the region of the $\nu_1+\nu_2, \nu_1+\nu_4, \nu_2+\nu_3$ and $\nu_3+\nu_4$ stretching–bending Tetrad. Experimental conditions: room temperature, sample pressures is 0.3 Torr, absorption path lengths is 3.75 m, numbers of scans are 1200 (see also Table 1). The lower trace of Fig. 1 shows corresponding simulated spectrum of $^{76}GeH_4$ (black) and $^{74}GeH_4$ (red).

Table 2
Number of the vibrational states of different symmetry in the polyads.

n(P_n)	m(A_1)	m(A_2)	m(E)	m(F_1)	m(F_2)	Name of polyad[a]	m[b]
0	1	0	0	0	0	Monad(1)	1
1	0	0	1	0	1	Dyad(2)	2
2	3	0	2	1	3	Pentad(5)	9
3	4	2	5	5	8	Octad(8)	24
4	11	2	14	13	20	Tetradecad(14)	60
5	18	11	28	34	43	Icosad(20)	134
6	41	20	58	71	90	Triacontad(30)	280
7	64	45	112	148	169	Tetracontad(40)	538
8	126	81	204	272	313	Pentacontakaipentad(55)	996

[a] Number of levels in parentheses.
[b] Total number of sublevels.

four stretch–bending levels, $\nu_1+\nu_2, \nu_1+\nu_4, \nu_2+\nu_3, \nu_3+\nu_4$, which consists of 8 sub–levels).

In the present paper we deal with the Tetrad of the $\nu_1+\nu_2, \nu_1+\nu_4, \nu_2+\nu_3$ and $\nu_3+\nu_4$ stretching–bending bands (eight ro–vibrational sub–bands) of the so–called Octad of the $^{76}GeH_4$ molecule. Another sixteen bending sub–bands of the Octad, which are located separately enough from the discussed stretching–bending bands, have been analysed in our resent paper [77], and (as the analysis showed) they can be omitted from the consideration in the present study. All eight sub–bands of the discussed Tetrad are strongly interact with each other. For that reason, analysis of the experimental spectra can be made correctly only in the frame of a model which takes into account numerous resonance interactions between all of these sub–bands. Moreover, the high symmetry of the GeH_4 molecule requires to use a special mathematical formalism (the theory of irreducible tensorial sets, see, e.g., [78–81]) for description of its ro–vibrational spectra. Application of the mentioned formalism to the $XY_4(T_d)$ molecules has been discussed in the spectroscopic literature many times (see, e.g., [82–86]). For that reason we present only briefly the main points necessary for understanding the procedure of calculations with the effective Hamiltonian of the XY_4 spherical top molecule.

As known from the general vibration-rotation theory [87–89], the Hamiltonian of an arbitrary polyatomic molecule can be reduced to a set of so–called effective Hamiltonians, or, in a more general case, to a set of effective operator matrices of the form, see, e.g., [90–93],

$$H^{vib.-rot.} = \sum_{a,b} |a\rangle \Big\langle b| H^{a,b}, \tag{1}$$

where $|a\rangle$ and $\langle b|$ are the basic vibrational functions; the operators $H^{a,b}$ depend on the rotational operators J_α only, and summation is performed in all degenerate and/or interacting vibrational states. When, as in our case, a molecule possesses a symmetry, Eq. (1) can be rewritten in the symmetrized form [84–86]:

$$\begin{aligned} H^{vib.-rot.} &= \sum_{v\gamma, v'r'\gamma'} \sum_{n\Gamma} \Big[(|v\gamma\rangle \otimes \langle v'r'\gamma'|)^{n\Gamma} \otimes H^{n\Gamma}_{v\gamma, v'r'\gamma'} \Big]^{A_1} \\ &\equiv \sum_{v\gamma, v'r'\gamma'} \sum_{n\Gamma} \sum_{\Omega K} \Big[(|v\gamma\rangle \otimes \langle v'r'\gamma'|)^{n\Gamma} \otimes R^{\Omega(K,n\Gamma)} \Big]^{A_1} Y^{\Omega(K,n\Gamma)}_{v\gamma, v'r'\gamma'}. \end{aligned} \tag{2}$$

In Eq. (2):

(a). $|v l\gamma\rangle$ are the symmetrized vibrational functions, γ are symmetries of these functions; $R_\sigma^{\Omega(K,n\Gamma)}$ are symmetrized rotational operators, and Ω is the total degree of the rotational operators J_α ($\alpha = x, y, z$) in the individual operator R; K is the rank of this operator (see, e.g., [94]), Γ is its symmetry in the T_d point symmetry group, and n distinguishes between possible different operators $R_\sigma^{\Omega(K,n\Gamma)}$ having the same values of Ω, K and Γ. The sign $\otimes$ denotes a tensorial product, and the values $Y^{\Omega(K,n\Gamma)}_{v_l\gamma,v_{l'}\gamma'}$ are different–type spectroscopic parameters.

(b). The symmetrized rotational operators, $R_\sigma^{\Omega(K,n\Gamma)}$, are determined as, [94],

$$R_\sigma^{\Omega(K,n\Gamma)} = \sum_m {}^{(K)}G^m_{n\Gamma\sigma} R_m^{\Omega(K)}, \tag{3}$$

where the operators $R_m^{\Omega(K)}$ are symmetrized in the SO(3) symmetry group rotational operator which can be constructed in accordance with the recurrence relation, [86,94]:

$$R^{\Omega+1(K+1)}_{\widetilde{m}} = \sum_{l=-1,0,1} C^{K+1\widetilde{m}}_{K\widetilde{m}-l,1l} R^{\Omega(K)}_{\widetilde{m}-l} R^{1(1)}_l, \tag{4}$$

where $C^{K+1\widetilde{m}}_{K\widetilde{m}-l,1l}$ are known Clebsch–Gordan coefficients, Ref. [80]. The irreducible rotational operators $R_m^{\Omega(K)}$ with $K < \Omega$ (in this case, the parity of both Ω, and K must be the same, [94]) are constructed as,

$$R_m^{\Omega(K)} = R_m^{\Omega=K(K)} \left(R^{2(0)}\right)^{(\Omega-K)/2}, \tag{5}$$

where the notation $R^{2(0)} = \left(J_x^2 + J_y^2 + J_z^2\right)$ is used. In this case, the first order and rank operators, $R_m^{1(1)}$ ($m = 0, \pm 1$) are determined as

$$\begin{aligned} R_1^{1(1)} &= -\tfrac{1}{\sqrt{2}}(J_x - iJ_y) \equiv -J_+, \\ R_{-1}^{1(1)} &= \tfrac{1}{\sqrt{2}}(J_x + iJ_y) \equiv J_-, \\ R_0^{1(1)} &= J_z \equiv J_0. \end{aligned} \tag{6}$$

The values ${}^{(K)}G^m_{n\Gamma\sigma}$ in Eq. (3) are so–called reduction matrix elements, which can be found in the literature (see, e.g., [83–96]).

4. Experimental spectrum and assignment of transitions

An overview of the recorded spectrum I is shown in the upper part of Fig. 1. One can see the clearly pronounced all three branches of the $\nu_1 + \nu_4$ and $\nu_3 + \nu_4$ bands and the R-branch of the weaker $\nu_2 + \nu_3$ band (the set of very weak line which are seen in the right part of the upper panel belongs to the $^{74}GeH_4$ species which was presented in the experimental spectrum in the amount of 11.5%). For the illustration of the quality of the results, small parts of the high resolution spectra II and III in the regions of the $\nu_3 + \nu_4$ and $\nu_2 + \nu_3$ bands are shown in the upper parts of Figs. 2 and 3.

Because the GeH_4 molecule is a spherical top with a symmetry isomorphic to the T_d point symmetry group, its transitions in absorption are allowed only between vibrational states $(v\Gamma)$ and $(v\prime\Gamma\prime)$ for which the relation (see, *e.g.*, [97])

$$\Gamma \otimes \Gamma\prime \in F_2$$

is fulfilled. Transitions between the vibrational states which do not satisfy the conditions, Eq. (7), are forbidden by the symmetry of the molecule and can appear in absorption spectra only because of resonance interactions with the allowed transitions.

Assignment of transitions of the $^{76}GeH_4$ isotopologue was made simultaneously with the fit of parameters $Y^{\Omega(K,n\Gamma)}_{v\gamma,v\prime\gamma\prime}$ of the effective Hamiltonian, Eq. (2) with the specially made computer code

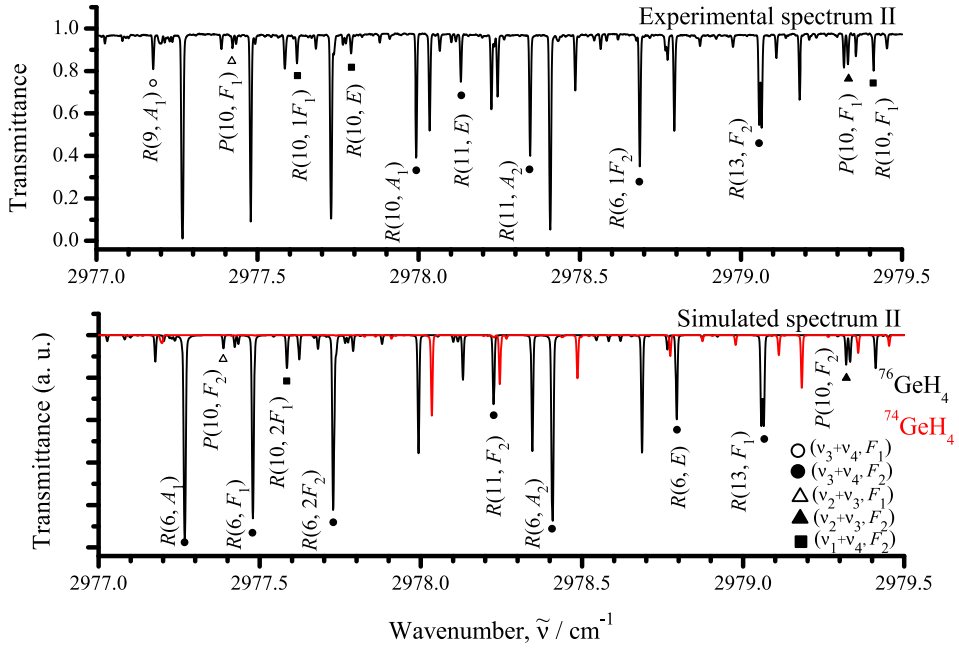

Fig. 2. Small part of the experimental (upper trace) high–resolution spectrum II of GeH_4 in the region of the $\nu_3 + \nu_4$ band (for the experimental details see Table 1). The lower trace shows corresponding simulated spectrum (see text for details) of the $^{76}GeH_4$ species (black). Ro–vibrational transitions of the $\nu_3 + \nu_4(F_2)$ and $\nu_3 + \nu_4(F_1)$, $\nu_2 + \nu_3(F_2)$ and $\nu_2 + \nu_3(F_1)$ and $\nu_1 + \nu_4(F_2)$ are marked by dark and open circles, dark and open triangles and dark squares, respectively. Considerably weaker red lines belong to the $^{76}GeH_4$ (11.5% in the sample used) species.

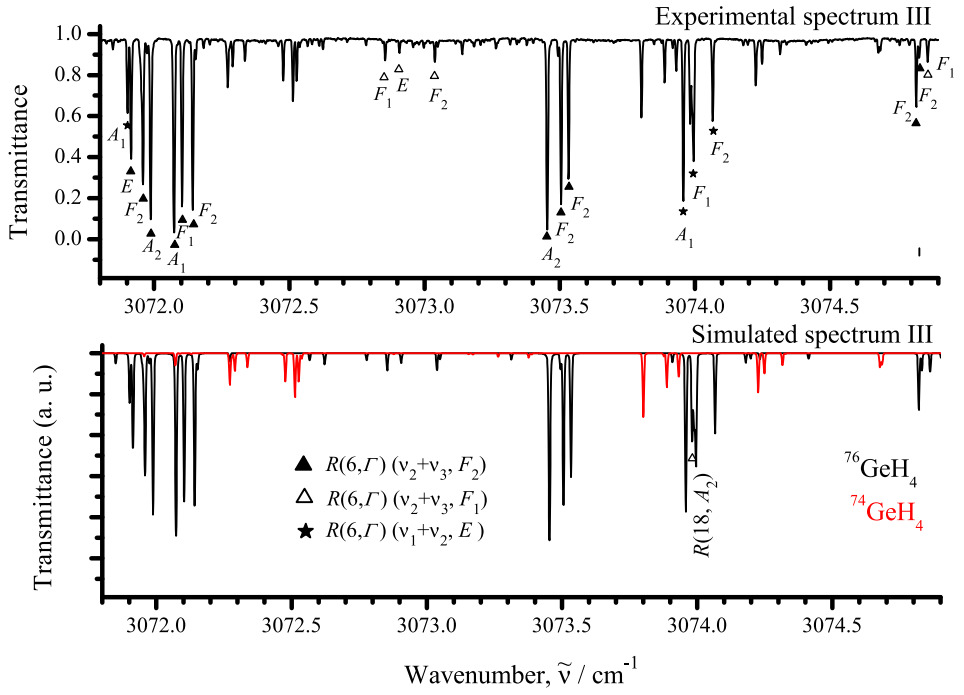

Fig. 3. Small part of the experimental (upper trace) high-resolution spectrum III of GeH_4 in the region of the $\nu_2 + \nu_3$ band (for the experimental details see Table 1). The lower trace shows corresponding (black) simulated spectrum (see text for details) of the $^{76}GeH_4$ species. The $R(6, \Gamma)$ clusters of the $\nu_2 + \nu_3(F_2)$, $\nu_2 + \nu_3(F_1)$ and $\nu_1 + \nu_2(E)$ bands are marked on the upper trace by dark and open triangles and dark stars, respectively. Considerably weaker red lines belong to the $^{74}GeH_4$ (11.5% in the sample used) species.

SPHETOM, [51]. As the result of the analysis, we assigned for the first time the 3595 transitions with the value of quantum number $J^{max} = 22$ to the eight sub–bands of the considered Tetrad of strongly interacting states. The obtained data is a considerable extension of the before known information about spectroscopic properties of the GeH_4 molecule. Complete list of 3595 assigned experimental transitions is presented as the Supplementary material to this paper, and, as an illustration, several small parts of this list are presented in Table 3 (column 7 of Table 3 presents line positions and column 8 show the values of corresponding transmittance values of lines; see also statistical information in Table 4). We would like to mark that for the convenience of the reader (because the reader in more familiar with the Dijon XTDS notation, [98], than with the notation of the SPHETOM code) notations of data in Table 3 (see columns 1–6) correspond to the XTDS one.

5. Ro–vibrational analysis and parameters of the effective Hamiltonian

The knowledge of the transition values allowed us to make a fit of parameters of the effective Hamiltonian (2). As was discussed above, at the first step of the analysis both an assignment and a preliminary fit of spectroscopic parameters were made using the SPHETOM code. However the final fit was made on the basis of the XTDS/Dijon software, [98]. The values of parameters obtained from the fit are presented in column 4 of Table 5 together with their 1σ confidence statistical intervals (the latter are given in parentheses). To give the possibility to use the obtained results by the reader, Tables 6–8 present the values of spectroscopic parameters of the lower ro–vibrational polyads of $^{76}GeH_4$ (the latter are reproduced from [51,77,99]).

The good quality of the fit can be seen in column 9 of Table 3, where differences between experimental line positions and line positions calculated with the parameters from Tables 5–8 are shown. In general, the value $d_{rms} = 6.81 \times 10^{-4}$ cm^{-1} (3595 initial line positions, 106 fitted parameters) is obtained (see also statistical information in Table 3). It is interesting to compare the results of the present fit of the Tetrad (as part of the Octad) of strongly interacting ro–vibrational bands with results of analogous fits of the Octad parameters of the related CH_4, Ref. [100], and SiH_4, [101], molecules. If one takes into account the $d_{rms} = 6.81 \times 10^{-4}$ cm^{-1} for the Tetrad (as part of the Octad) and the $d_{rms} = 6.43 \times 10^{-4}$ cm^{-1} from Ref. [77] for the another sixteen bending bands of the Octad and compare these values with corresponding $d_{rms} = 35 \times 10^{-4}$ cm^{-1} from Ref. [100] for the Octad of CH_4 and/or $d_{rms} = 46 \times 10^{-4}$ cm^{-1} from Ref. [101] for the Octad of SiH_4, then one can see about 5–7 times higher reproduction of the experimental data in the present study in comparison with analogous analysis in Refs. [100,101]. Because of very complicated picture of numerous resonance interactions in the Octad spectra (as an illustration, see Fig. 4 where the diagram of ro–vibrational energy levels for the Octad of $^{76}GeH_4$ is shown; part of the Octad diagram corresponding the triply excited deformational states was calculated with the parameters from [77]), this fact indicates the better description of resonance interactions in this study in comparison with corresponding analysis of the Octad regions in relative CH_4 and SiH_4 molecules. Also to illustrate the quality of the results, bottom panels of Figs. 1–3 show the simulated spectra which were obtained with the parameters from Tables 5–8. In this case, relative line strengths have been calculated with the use of three effective dipole moment parameters (one main effective dipole moment parameter for one of three F_2-symmetry band). Relative values of these three main effective dipole moment parameters have been estimated from the specially measured 12 line strengths in the experimental spectrum and, as was found, approximately relate as 0.0045: (-0.011):0.018 for the sub–bands $\nu_1 + \nu_4(F_2)$, $\nu_2 + \nu_3(F_2)$ and $\nu_3 + \nu_4(F_2)$. A Voigt profile was used in calculations. Weak lines of the $^{74}GeH_4$ species, which are presented in experimental spectra, are marked in the simulated spectra by red. In this case, parameters of the effective Hamiltonian of

Table 3
Part of list of transitions assigned to the $\nu_1+\nu_2$, $\nu_1+\nu_4$, $\nu_2+\nu_3$ and $\nu_3+\nu_4$ ro–vibrational bands.

J	γ	n	J'	γ'	n'	ν^{exp} in cm^{-1}	Transmitt. in %	$\delta\times10^4$ in cm^{-1}	Spectrum	Band
1	2	3	4	5	6	7	8	9	10	11
6	F_2	63	7	F_1	1	2867.7556	96.8	0.0	III	$\nu_3+\nu_4, F_2$
6	E	42	7	E	1	2867.8683	57.9	1.7	II	$\nu_3+\nu_4, F_2$
6	F_1	61	7	F_2	2	2867.9327	69.2	1.0	II	$\nu_3+\nu_4, F_2$
8	F_1	82	9	F_2	2	2867.9460	87.7	−3.7	III	$\nu_3+\nu_4, E$
6	F_1	61	7	F_2	1	2867.9520	89.8	−0.7	III	$\nu_3+\nu_4, F_2$
6	A_1	23	7	A_2	1	2868.0238	56.9	1.1	II	$\nu_3+\nu_4, F_2$
9	F_1	101	10	F_2	2	2868.1729	70.9	−0.0	III	$\nu_3+\nu_4, F_1$
14	F_2	158	15	F_1	3	2868.2422	90.1	-5.2	II	$\nu_3+\nu_4, F_2$
8	A_1	29	9	A_2	1	2868.3366	92.9	-0.2	II	$\nu_3+\nu_4, E$
17	F_1	170	17	F_2	2	2868.3489	92.0	-0.9	III	$\nu_3+\nu_4, F_2$
15	F_2	140	15	F_1	3	2868.5460	86.2	-1.9	III	$\nu_1+\nu_4, F_2$
15	E	92	15	E	2	2868.5720	90.9	-7.1	III	$\nu_1+\nu_4, F_2$
14	E	107	15	E	2	2868.9893	94.1	-0.7	II	$\nu_3+\nu_4, F_2$
9	F_2	100	10	F_1	2	2869.2746	79.4	1.0	III	$\nu_3+\nu_4, F_2$
9	F_2	100	10	F_1	1	2869.3133	76.9	1.8	III	$\nu_3+\nu_4, F_2$
8	A_2	27	9	A_1	1	2869.3372	59.0	-4.8	III	$\nu_1+\nu_4, F_2$
17	E	113	17	E	1	2869.3639	88.9	-1.8	III	$\nu_3+\nu_4, F_2$
17	F_2	168	17	F_1	2	2869.3751	87.2	-1.7	III	$\nu_3+\nu_4, F_2$
17	A_2	57	17	A_1	1	2869.3957	79.4	-0.1	III	$\nu_3+\nu_4, F_2$
10	F_2	94	9	F_1	2	2940.3742	93.1	-0.2	I	$\nu_3+\nu_4, F_1$
6	F_2	72	6	F_1	1	2940.4604	78.5	-2.6	I	$\nu_1+\nu_4, F_2$
6	A_1	26	6	A_2	1	2940.6517	44.9	-2.2	II	$\nu_3+\nu_4, F_2$
7	A_1	27	7	A_2	1	2940.7059	64.2	-3.6	II	$\nu_3+\nu_4, F_2$
6	F_1	71	6	F_2	2	2940.7960	90.1	-1.0	II	$\nu_3+\nu_4, F_2$
6	F_1	71	6	F_2	1	2940.8070	64.8	-1.4	II	$\nu_3+\nu_4, F_2$
10	A_2	31	9	A_1	1	2940.8382	87.7	1.7	II	$\nu_3+\nu_4, F_1$
10	F_2	95	9	F_1	2	2940.8713	85.2	3.4	I	$\nu_3+\nu_4, F_1$
10	E	64	9	E	1	2940.8835	88.4	2.4	II	$\nu_3+\nu_4, F_1$
6	A_1	27	6	A_2	1	2940.8952	75.1	3.2	II	$\nu_3+\nu_4, F_1$
7	F_1	83	7	F_2	2	2940.9762	87.6	-1.4	II	$\nu_3+\nu_4, F_2$
6	E	49	6	E	1	2940.9878	70.4	-5.8	II	$\nu_3+\nu_4, F_2$
7	F_1	83	7	F_2	1	2940.9957	89.7	-0.9	I	$\nu_3+\nu_4, F_2$
7	E	53	7	E	1	2941.0801	91.9	0.0	II	$\nu_3+\nu_4, F_2$
6	A_2	24	6	A_1	1	2941.1442	48.6	-0.7	II	$\nu_3+\nu_4, F_1$
8	E	63	8	E	2	2941.2150	90.1	-2.4	I	$\nu_3+\nu_4, F_2$
6	F_2	73	6	F_1	1	2941.3267	66.4	3.8	I	$\nu_3+\nu_4, F_1$
9	F_1	90	8	F_2	1	2941.3352	89.2	-4.8	III	$\nu_1+\nu_4, F_2$
9	E	58	8	E	2	2941.3465	91.0	-1.9	III	$\nu_3+\nu_4, F_1$
9	F_1	91	8	F_2	1	2941.3765	91.9	1.1	III	$\nu_3+\nu_4, F_1$
2	F_2	27	1	F_1	1	2941.3884	73.3	-2.3	II	$\nu_3+\nu_4, F_2$
8	F_1	88	7	F_2	2	2966.2723	87.2	2.4	III	$\nu_3+\nu_4, F_1$
8	F_1	88	7	F_2	1	2966.2916	79.3	0.5	III	$\nu_3+\nu_4, F_1$
11	F_1	138	12	F_2	1	2966.3210	78.9	0.1	III	$\nu_2+\nu_3, F_1$
11	F_2	136	12	F_1	2	2966.3264	79.2	-3.0	III	$\nu_2+\nu_3, F_1$
8	F_1	89	7	F_2	2	2966.4244	79.0	-1.2	III	$\nu_1+\nu_4, F_2$
12	E	105	13	E	2	2966.4611	81.2	12.8	III	$\nu_1+\nu_2, E$
12	F_2	159	13	F_1	4	2966.4977	61.6	4.6	III	$\nu_2+\nu_3, F_2$
5	A_2	22	4	A_1	1	2966.5341	57.2	4.3	II	$\nu_3+\nu_4, F_1$
9	F_2	96	8	F_1	1	2966.5641	93.7	-1.7	I	$\nu_3+\nu_4, F_2$
8	E	62	7	E	1	2966.5720	93.0	-0.2	II	$\nu_3+\nu_4, F_2$
5	E	42	4	E	1	2966.5911	72.7	-6.1	I	$\nu_3+\nu_4, F_1$
11	E	92	12	E	2	2966.6107	91.3	-2.6	III	$\nu_2+\nu_3, F_2$
11	F_1	139	12	F_2	2	2966.6290	88.1	-2.6	III	$\nu_2+\nu_3, F_2$
9	F_1	97	8	F_2	1	2966.7628	73.4	0.3	II	$\nu_3+\nu_4, F_2$
12	A_1	55	13	A_2	1	2966.8875	78.5	-5.2	III	$\nu_2+\nu_3, F_1$
12	F_1	157	13	F_2	3	2966.9371	75.2	1.3	III	$\nu_2+\nu_3, F_1$
12	E	106	13	E	2	2966.9547	77.9	-4.1	III	$\nu_2+\nu_3, F_1$
9	F_1	98	8	F_2	1	2966.9680	73.0	-1.7	III	$\nu_3+\nu_4, F_2$
10	E	85	10	E	2	3031.4412	91.7	0.4	II	$\nu_2+\nu_3, F_2$
9	F_2	113	9	F_1	3	3031.4648	67.9	-5.4	III	$\nu_2+\nu_3, F_2$
11	F_2	138	11	F_1	2	3031.4729	48.9	-4.6	III	$\nu_2+\nu_3, F_1$
10	F_1	126	10	F_2	3	3031.4805	37.3	2.4	III	$\nu_2+\nu_3, F_2$
8	A_2	33	8	A_1	1	3031.4899	75.0	-5.4	II	$\nu_2+\nu_3, F_1$
9	F_2	113	9	F_1	2	3031.4899	75.0	-8.1	II	$\nu_2+\nu_3, F_2$
14	E	111	13	E	1	3031.5111	68.4	6.6	III	$\nu_3+\nu_4, F_1$
9	E	75	9	E	1	3031.5377	76.0	-5.5	II	$\nu_2+\nu_3, F_1$
9	F_1	116	9	F_2	2	3031.5607	80.4	7.2	II	$\nu_2+\nu_3, F_2$
7	F_1	91	7	F_2	1	3031.5607	80.4	-0.6	II	$\nu_2+\nu_3, F_2$
9	A_1	38	9	A_2	1	3031.5692	78.4	4.1	II	$\nu_2+\nu_3, F_2$
9	F_2	114	9	F_1	3	3031.5801	90.3	-7.8	II	$\nu_2+\nu_3, F_2$
8	F_2	104	8	F_1	2	3031.5905	87.0	-2.5	II	$\nu_2+\nu_3, F_2$
9	F_2	114	9	F_1	2	3031.6053	61.7	-9.3	III	$\nu_2+\nu_3, F_2$

Table 3 (*continued*)

J	γ	n	$J\prime$	$\gamma\prime$	$n\prime$	ν^{exp} in cm^{-1}	Transmitt. in %	$\delta \times 10^4$ in cm^{-1}	Spectrum	Band
1	2	3	4	5	6	7	8	9	10	11
8	F_2	104	8	F_1	1	3031.6267	82.4	-3.3	III	$\nu_2+\nu_3,F_2$
8	F_1	100	8	F_2	1	3031.6391	80.1	1.5	II	$\nu_2+\nu_3,F_1$
16	E	119	15	E	2	3031.7028	52.3	-7.4	III	$\nu_1+\nu_4,F_2$
7	F_1	92	7	F_2	2	3031.7382	83.2	-7.8	II	$\nu_2+\nu_3,F_1$
6	F_1	77	6	F_2	2	3031.7664	66.6	2.3	III	$\nu_2+\nu_3,F_1$
6	F_1	77	6	F_2	1	3031.7775	88.7	2.3	II	$\nu_2+\nu_3,F_1$

Table 4
Statistical information for the $\nu_1+\nu_2(E)$, $\nu_1+\nu_4(F_2)$, $\nu_2+\nu_3(F_1,F_2)$ and $\nu_3+\nu_4(A_1,E,F_1,F_2)$ bands of $^{76}GeH_4$.

Band	Energy[a]/cm^{-1}	J^{max}	$N_{tr}^{b)}$	$N_l^{c)}$	$m_1^{d)}$	$m_2^{d)}$	$m_3^{d)}$
1	2	3	4	5	6	7	8
$\nu_1+\nu_2(E)$	3034.3769	16	86	56	34.9	19.8	45.3
$\nu_1+\nu_4(F_2)$	2925.3459	21	521	253	65.3	20.4	14.3
$\nu_2+\nu_3(F_1)$	3032.8684	20	325	186	47.1	22.8	30.1
$\nu_2+\nu_3(F_2)$	3033.1965	19	537	280	39.5	19.6	40.9
$\nu_3+\nu_4(A_1)$	2926.9062	6	4	2	100.0	0.0	0.0
$\nu_3+\nu_4(E)$	2924.9988	18	124	64	74.2	17.7	8.1
$\nu_3+\nu_4(F_1)$	2924.2417	20	937	446	76.1	16.3	7.6
$\nu_3+\nu_4(F_2)$	2927.0022	22	1061	530	82.5	13.3	4.2
Total N_{tr}			3595				
Total N_l				1817			
d_{rms}	$6.81\times10^{-4}cm^{-1}$						

[a)] Value of the upper vibrational energy.
[b)] N_{tr} is the number of assigned transitions.
[c)] N_l is the number of obtained upper-state energies.
[d)] Here $m_i = n_i/N_{tr}\times100$ % (i = 1, 2, 3); n_1, n_2, and n_3 are the numbers of transitions for which the differences $\delta = \nu^{exp} - \nu^{calc}$ satisfy the conditions $\delta \le 4\times10^{-4}$ cm^{-1}, 4

Table 5
Spectroscopic parameters $Y^{\Omega(K,n\Gamma)}_{\nu\gamma,\nu'\gamma'}$ of the (1100)/(1001)/(0110)/(0011) vibrational states of $^{76}GeH_4$ (in cm^{-1})[a]

(ν,γ)	(ν',γ')	$\Omega(K,n\Gamma)$	$^{76}GeH_4$	(ν,γ)	(ν',γ')	$\Omega(K,n\Gamma)$	$^{76}GeH_4$
1	2	3	4	1	2	3	4
(1100,E)	(1100,E)	0($0,A_1$)	-6.3763(11)	(0110,F_1)	(0110,F_1)	0($0,A_1$)	-8.157465(45)
	(1100,E)	2($0,A_1$)10^3	1.8533(98)		(0110,F_1)	2($0,A_1$)10^5	−5.104(48)
	(1100,E)	2($2,E$)10^3	1.9441(85)		(0110,F_1)	2($2,F_2$)10^5	3.91(18)
	(1100,E)	4($0,A_1$)10^7	−3.369(31)		(0110,F_1)	3($1,F_1$)10^6	6.249(17)
	(1100,E)	4($2,E$)10^7	8.802(24)	(0110,F_1)	(0110,F_2)	1($1,F_1$)10^3	-6.04(11)
(1100,E)	(1001,F_2)	1($1,F_1$)10^1	1.3999(53)		(0110,F_2)	2($2,F_2$)10^4	−5.092(15)
	(1001,F_2)	2($2,F_2$)10^3	−1.088(12)		(0110,F_2)	3($3,F_1$)10^6	2.8088(91)
	(1001,F_2)	3($1,F_1$)10^5	-5.0928(92)		(0110,F_2)	3($3,F_2$)10^6	−9.113(32)
(1100,E)	(0110,F_1)	1($1,F_1$)10^2	3.088(50)	(0110,F_2)	(0110,F_2)	0($0,A_1$)	-7.7296(13)
	(0110,F_1)	2($2,F_2$)10^4	−3.973(64)		(0110,F_2)	1($1,F_1$)10^2	−4.423(39)
	(0110,F_1)	3($1,F_1$)10^5	1.2780(96)		(0110,F_2)	2($2,E$)10^4	−1.006(12)
(1100,E)	(0110,F_2)	1($1,F_1$)10^2	−2.147(57)		(0110,F_2)	2($2,F_2$)10^4	−1.076(14)
	(0110,F_2)	2($2,F_2$)10^3	−1.600(10)		(0110,F_2)	3($1,F_1$)10^6	7.789(29)
	(0110,F_2)	3($1,F_1$)10^6	−1.866(81)	(0110,F_1)	(0011,E)	1($1,F_1$)10^3	−9.898(39)
	(0110,F_2)	3($3,F_1$)10^5	3.3378(86)		(0011,E)	3($1,F_1$)10^6	−4.181(18)
	(0110,F_2)	3($3,F_2$)10^6	2.573(49)	(0110,F_1)	(0011,F_1)	0($0,A_1$)	6.41838(33)
	(0110,F_2)	4($2,F_2$)10^7	3.423(10)		(0011,F_1)	1($1,F_1$)10^2	4.7828(88)
(1100,E)	(0011,E)	0($0,A_1$)	−4.027(14)		(0011,F_1)	2($0,A_1$)10^4	−2.746(13)
	(0011,E)	2($0,A_1$)10^3	1.015(10)		(0011,F_1)	2($2,E$)10^4	−4.254(11)
(1100,E)	(0011,F_1)	1($1,F_1$)10^2	−7.894(57)		(0011,F_1)	2($2,F_2$)10^4	4.8693(90)
	(0011,F_1)	2($2,F_2$)10^4	5.63(10)	(0110,F_1)	(0011,F_2)	1($1,F_1$)10^2	-4.9670(68)
(1100,E)	(0011,F_2)	1($1,F_1$)10^1	-1.4904(77)		(0011,F_2)	2($2,E$)10^4	−5.660(10)
	(0011,F_2)	2($2,F_2$)10^3	−3.534(12)	(0110,F_2)	(0011,E)	1($1,F_1$)10^2	7.413(16)
	(0011,F_2)	3($1,F_1$)10^5	−2.440(16)	(0110,F_2)	(0011,F_1)	1($1,F_1$)10^2	3.374(18)
(1001,F_2)	(1001,F_2)	0($0,A_1$)	-4.7198(14)		(0011,F_1)	2($2,E$)10^4	4.238(11)
	(1001,F_2)	1($1,F_1$)10^2	-3.9054(78)		(0011,F_1)	2($2,F_2$)10^4	−4.786(24)
	(1001,F_2)	2($0,A_1$)10^3	-1.5382(65)	(0110,F_2)	(0011,F_2)	0($0,A_1$)	2.0053(51)
	(1001,F_2)	2($2,E$)10^3	2.2870(97)		(0011,F_2)	1($1,F_1$)10^2	−3.196(17)

(*continued on next page*)

Table 5 (*continued*)

(v,γ) 1	$(v\prime,\gamma\prime)$ 2	$\Omega(K,n\Gamma)$ 3	$^{76}GeH_4$ 4	(v,γ) 1	$(v\prime,\gamma\prime)$ 2	$\Omega(K,n\Gamma)$ 3	$^{76}GeH_4$ 4
	(1001,F_2)	2(2,F_2)10^3	-1.6730(71)	(0011,A_1)	(0011,A_1)	0(0,A_1)	-4.153074(28)
	(1001,F_2)	3(1,F_1)10^5	3.2822(30)	(0011,A_1)	(0011,F_1)	1(1,F_1)10^2	2.38272(82)
	(1001,F_2)	3(3,F_1)10^5	2.6637(39)	(0011,A_1)	(0011,F_2)	2(2,F_2)10^4	2.2905(90)
	(1001,F_2)	4(0,A_1)10^6	-1.3959(25)	(0011,E)	(0011,E)	0(0,A_1)	-5.9120(11)
	(1001,F_2)	4(2,E)10^7	−5.432(20)		(0011,E)	2(0,A_1)10^4	3.1051(92)
	(1001,F_2)	4(2,F_2)10^7	7.107(13)		(0011,E)	2(2,E)10^4	-3.0886(52)
(1001,F_2)	(0110,F_1)	1(1,F_1)10^2	−8.087(73)		(0011,E)	3(3,A_2)10^6	-2.6839(95)
	(0110,F_1)	2(2,E)10^4	−8.075(99)	(0011,E)	(0011,F_1)	1(1,F_1)10^3	−4.648(14)
	(0110,F_1)	3(1,F_1)10^6	−8.586(83)		(0011,F_1)	2(2,F_2)10^4	4.116(13)
	(0110,F_1)	3(3,A_2)10^6	−9.126(40)	(0011,E)	(0011,F_2)	1(1,F_1)10^2	-3.9225(22)
(1001,F_2)	(0110,F_2)	0(0,A_1)	−5.111(14)		(0011,F_2)	2(2,F_2)10^4	7.200(16)
	(0110,F_2)	1(1,F_1)10^2	3.87(11)	(0011,F_1)	(0011,F_1)	0(0,A_1)	-6.436982(40)
	(0110,F_2)	2(0,A_1)10^3	1.084(10)		(0011,F_1)	1(1,F_1)10^2	-2.19084(57)
	(0110,F_2)	2(2,E)10^3	-3.8173(92)		(0011,F_1)	2(2,E)10^4	1.4329(43)
	(0110,F_2)	2(2,F_2)10^4	8.93(15)		(0011,F_1)	2(2,F_2)10^5	-9.43(18)
	(0110,F_2)	3(1,F_1)10^5	−2.673(18)	(0011,F_1)	(0011,F_2)	1(1,F_1)10^2	1.285(19)
	(0110,F_2)	3(3,F_1)10^6	−5.533(86)		(0011,F_2)	2(2,E)10^5	4.127(17)
(1001,F_2)	(0011,A_1)	2(2,F_2)10^5	-3.43(78)		(0011,F_2)	2(2,F_2)10^5	4.33(15)
(1001,F_2)	(0011,E)	1(1,F_1)10^2	−1.583(60)		(0011,F_2)	3(1,F_1)10^6	2.0717(73)
	(0011,E)	2(2,F_2)10^3	2.0484(93)	(0011,F_2)	(0011,F_2)	0(0,A_1)	-4.72947(23)
	(0011,E)	3(1,F_1)10^5	−2.619(15)		(0011,F_2)	1(1,F_1)10^1	1.1669(38)
(1001,F_2)	(0011,F_1)	1(1,F_1)10^2	3.101(70)		(0011,F_2)	3(1,F_1)10^6	−1.535(18)
	(0011,F_1)	2(2,F_2)10^4	−4.904(99)				
(1001,F_2)	(0011,F_2)	0(0,A_1)10^1	7.2465(31)				
	(0011,F_2)	2(0,A_1)10^4	−6.997(76)				
	(0011,F_2)	2(2,E)10^3	-1.6066(88)				
	(0011,F_2)	2(2,F_2)10^4	-7.60(12)				
	(0011,F_2)	3(1,F_1)10^6	-1.41(23)				

[a] Values in parenthesis are 1σ statistical standard errors.

Table 6
Spectroscopic parameters $Y^{\Omega(K,n\Gamma)}_{v\gamma;v\prime\gamma\prime}$ of the ground state of $^{76}GeH_4$ (in cm^{-1})

(v,γ) 1	$(v\prime,\gamma\prime)$ 2	$\Omega(K,n\Gamma)$ 3	$^{76}GeH_4$[a] 4
$(0000,A_1)$	$(0000,A_1)$	$2(0,A_1)$	2.695870305
$(0000,A_1)$	$(0000,A_1)$	$4(0,A_1)10^4$	-0.3341682
$(0000,A_1)$	$(0000,A_1)$	$4(4,A_1)10^5$	-0.1547079
$(0000,A_1)$	$(0000,A_1)$	$6(0,A_1)10^8$	0.114368
$(0000,A_1)$	$(0000,A_1)$	$6(4,A_1)10^{10}$	-0.51075
$(0000,A_1)$	$(0000,A_1)$	$6(6,A_1)10^{10}$	-0.15638

[a] Reproduced from Ref. [51].

$^{74}GeH_4$ have been estimated in accordance with the isotopic substitution theory, [102–104], and the effective dipole moment parameters of $^{74}GeH_4$ have been taken as equal to the corresponding parameters of the $^{76}GeH_4$ molecule. From a comparison of the top and bottom parts of Figs. 1–3, one can see good correspondence between the experimental and simulated spectra. To give the reader a possibility to appreciate the quality of the results, Fig. 5 shows the fit residuals for transition values as a function of the quantum number J.

As was mentioned above, very complicated picture of the recorded spectra is a consequence of the presence of numerous and strong resonance interactions between bands located in the discussed spectral range. The following facts can be noted as evidence of this:

(1) An appearance in spectra a number of "forbidden" transitions belonging to the five vibrational sub–bands of the F_1, E, A_1 and A_2 symmetry which are forbidden in absorption because of the T_d symmetry of the GeH_4 molecule, but nevertheless are seen in the spectra because of the presence of strong resonance interactions with the three F_2-type symmetry $\nu_1+\nu_4(F_2), \nu_2+\nu_3(F_2)$ and $\nu_3+\nu_4(F_2)$ bands. In this case, as is seen from Table 4 and the Supplementary material,
   (a) in general, the number of such "forbidden" transitions is almost the same as the number of "allowed" transitions of the $\nu_1+\nu_4(F_2), \nu_2+\nu_3(F_2)$ and $\nu_3+\nu_4(F_2)$ bands,
   (b) strengths of "forbidden" transitions are comparable with the strengths of "allowed" transitions in many cases.

(2) As follows from the analysis, the obtained set of the effective Hamiltonian parameters (see Table 5) reproduces the initial experimental line positions with an accuracy comparable with the experimental uncertainties. At the same time, as the analysis showed, this is possible only if different kind resonance interaction parameters are taken into account in the used mathematical model. Attempt to eliminate from the model resonance interaction parameters of the Tetad (see Table 5), even keeping interaction parameters of the lower polyads in the model (see Tables 7,8), leads to the considerably worse theoretical reproduction of the initial experimental line positions: the value of the d_{rms} deviation is increased up to 0.2723 cm^{-1}, *i.e.*, more than 400 times in comparison with the value of d_{rms}= 6.81 $\times 10^{-4}$ cm^{-1} which corresponds to our results.

Table 7
Spectroscopic parameters $Y^{\Omega(K,n\Gamma)}_{v\gamma;v\gamma'}$ of the (0100)/(0001) vibrational states of $^{76}GeH_4$ (in cm^{-1})[a)]

(v,γ) 1	(v',γ') 2	$\Omega(K,n\Gamma)$ 3	$^{76}GeH_4$ 4
$(0100,E)$	$(0100,E)$	$0(0,A_1)$	929.9130275
	$(0100,E)$	$2(2,E)10^1$	-0.1078743
	$(0100,E)$	$3(3,A_2)10^4$	0.22618
	$(0100,E)$	$4(0,A_1)10^6$	-0.4052
	$(0100,E)$	$4(2,E)10^6$	-0.31077
	$(0100,E)$	$4(4,A_1)10^7$	0.134
	$(0100,E)$	$4(4,E)10^6$	-0.12583
$(0100,E)$	$(0001,F_2)$	$1(1,F_1)$	-4.503062
	$(0001,F_2)$	$2(2,F_2)$	-0.0213168
	$(0001,F_2)$	$3(1,F_1)10^3$	-0.1179267
	$(0001,F_2)$	$3(3,F_2)10^4$	0.138096
	$(0001,F_2)$	$4(2,F_2)10^6$	-0.2122
	$(0001,F_2)$	$4(4,F_1)10^6$	-0.18552
	$(0001,F_2)$	$4(4,F_2)10^6$	-0.209879
	$(0001,F_2)$	$5(1,F_1)10^8$	-0.23013
	$(0001,F_2)$	$5(3,F_1)10^8$	0.13677
	$(0001,F_2)$	$5(3,F_2)10^9$	0.5885
$(0001,F_2)$	$(0001,F_2)$	$0(0,A_1)$	820.3270025
	$(0001,F_2)$	$1(1,F_1)$	6.39186203
	$(0001,F_2)$	$2(0,A_1)10^2$	0.1060455
	$(0001,F_2)$	$2(2,E)10^2$	-0.14849411
	$(0001,F_2)$	$2(2,F_2)$	-0.0106923
	$(0001,F_2)$	$3(1,F_1)10^4$	0.70545
	$(0001,F_2)$	$3(3,F_1)10^4$	-0.47902
	$(0001,F_2)$	$4(0,A_1)10^6$	-0.3653
	$(0001,F_2)$	$4(2,F_2)10^6$	-0.3519
	$(0001,F_2)$	$4(4,A_1)10^7$	-0.6407
	$(0001,F_2)$	$5(1,F_1)10^8$	0.25953
	$(0001,F_2)$	$5(3,F_1)10^8$	-0.16967
	$(0001,F_2)$	$6(0,A_1)10^{10}$	0.4276

[a)] Reproduced from Ref. [51].

Table 8
Spectroscopic parameters $Y^{\Omega(K,n\Gamma)}_{v\gamma;v\gamma'}$ of the set of interacting vibrational states (1000)/(0010) in $^{76}GeH_4$ (in cm^{-1})[a)]

(v,γ) 1	(v',γ') 2	$\Omega(K,n\Gamma)$ 3	$^{76}GeH_4$ 4
$(1000,A_1)$	$(1000,A_1)$	$0(0,0A_1)$	2110.691769(11)
	$(1000,A_1)$	$2(0,0A_1)$	-0.01799331(14)
	$(1000,A_1)$	$4(0,0A_1)10^4$	-0.0019367(28)
	$(1000,A_1)$	$4(4,0A_1)10^5$	-0.000420(12)
$(1000,A_1)$	$(0010,F_2)$	$2(2,0F_2)10^2$	-0.8076987(80)
	$(0010,F_2)$	$3(3,0F_2)10^5$	-0.14853(63)
	$(0010,F_2)$	$4(2,0F_2)10^6$	-0.10836(66)
	$(0010,F_2)$	$4(4,0F_2)10^6$	-0.15996(77)
	$(0010,F_2)$	$5(5,0F_2)10^9$	0.2873(90)
$(0010,F_2)$	$(0010,F_2)$	$0(0,0A_1)$	2110.7323088(58)
	$(0010,F_2)$	$1(1,0F_1)$	-0.5686669(15)
	$(0010,F_2)$	$2(0,0A_1)$	-0.014686010(52)
	$(0010,F_2)$	$2(2,0E)10^2$	0.2234550(91)
	$(0010,F_2)$	$2(2,0F_2)10^2$	-0.447832(10)
	$(0010,F_2)$	$3(1,0F_1)10^5$	-0.76349(41)
	$(0010,F_2)$	$3(3,0F_1)10^5$	-0.64671(23)
	$(0010,F_2)$	$4(0,0A_1)10^4$	0.0
	$(0010,F_2)$	$4(2,0E)10^7$	0.9537(34)
	$(0010,F_2)$	$4(2,0F_2)10^7$	-0.6775(34)
	$(0010,F_2)$	$4(4,0A_1)10^5$	0.0010694(64)
	$(0010,F_2)$	$4(4,0E)10^7$	0.1407(50)
	$(0010,F_2)$	$4(4,0F_2)10^6$	-0.20740(32)
	$(0010,F_2)$	$5(1,0F_1)10^9$	-0.558(12)
	$(0010,F_2)$	$5(5,0F_1)10^9$	0.370(11)
	$(0010,F_2)$	$5(5,1F_1)10^9$	-0.639(20)

[a)] Reproduced from Ref. [99].

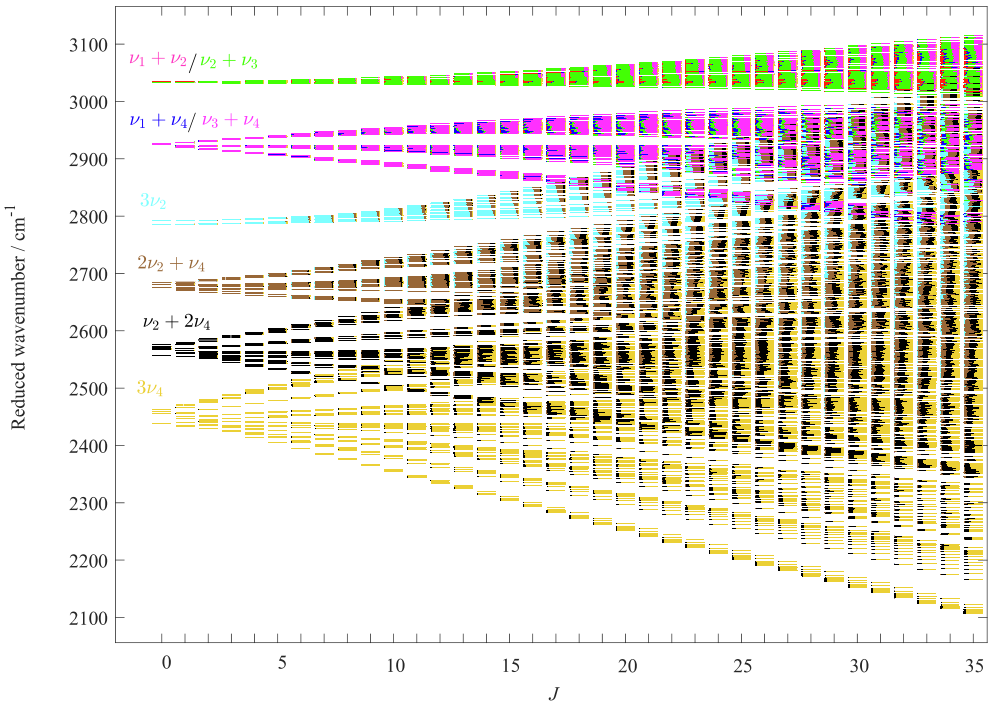

Fig. 4. Calculated reduced ro–vibrational energy levels (see text) for the Octad of $^{76}GeH_4$. The colors indicating the mixings of the different normal vibrations where obtained through projection on the initial basis set (color online). The energies have been calculated from the constants given in Tables 5–8. In order to suppress most of the J-slope, the calculated energies have been reduced by $(BJ(J+1)-DJ^2(J+1)^2+HJ^4(J+1)^4)$.

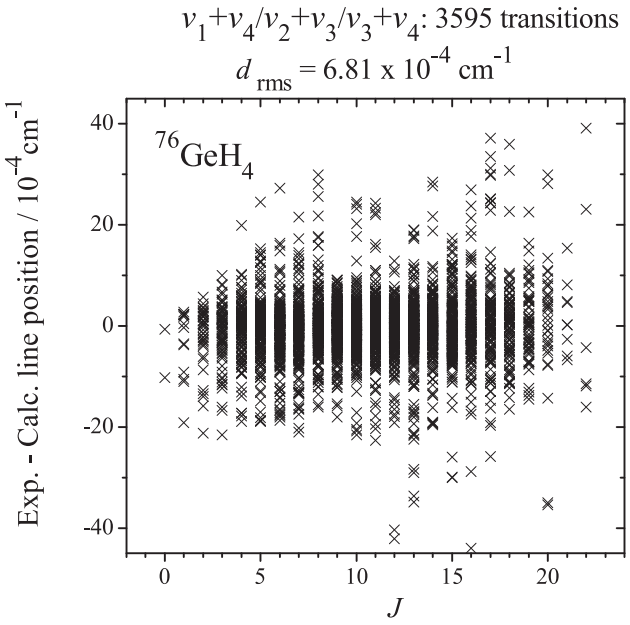

Fig. 5. Observed minus calculated line positions and fit statistics for the stretching–bending Tetrad $(\nu_1+\nu_2, \nu_1+\nu_4, \nu_2+\nu_3$ and $\nu_3+\nu_4)$ of $^{76}GeH_4$.

(3) Rendered result of the influence of the resonance interactions on the ro–vibrational states is brightly seen in Fig. 4 where the color segmentation of each tick (individual tick corresponds to individual ro–vibrational state) indicates that any ro–vibrational state is a mixture of states belonging to different vibrational states of the Octad.

6. Conclusion

We performed the first analysis of the high resolution IR spectra of germane (specially enriched up to 88.1% of $^{76}GeH_4$ in the sample) in the region of 2700–3200 cm^{-1} where the bending–stretching Tetrad ($\nu_1+\nu_2, \nu_1+\nu_4$, $\nu_2+\nu_3$ and $\nu_3+\nu_4$ bands) of the ro–vibrational Octad of germane is located. The 3595 transitions with the maximum value of the upper quantum numbers $J^{max}=22$ were assigned for the first time to the eight sub–bands of this Tetrad. A set of 106 spectroscopic parameters obtained from a weighted least square fit reproduces the initial 3595 experimental transitions with the d_{rms}= 6.81 $\times 10^{-4}$ cm^{-1}.

Declaration of Competing Interest

The authors declare that they have no known competing financial interests or personal relationships that could have appeared to influence the work reported in this paper.

Acknowledgments

The study was financially supported by Tomsk Polytechnic University development program.

Appendix A. Supplementary material

Supplementary data associated with this article can be found, in the online version, at https://doi.org/10.1016/j.saa.2022.121135.

References

[1] M. Agostini, M. Allardt, E. Andreotti, A.M. Bakalyarov, M. Balata, I. Barabanov, et al., The background in the $0\nu\beta\beta$ experiment GERDA, Eur. Phys. J. 74 (2014) 1–25, https://doi.org/10.1140/epjc/s10052-014-2764-z.

[2] E.E. Haller, Germanium: From its discovery to SiGe devices, Mater. Sci. Semicond. Process. 9 (2006) 408–422, https://doi.org/10.1016/j.mssp.2006.08.063.

[3] R.J. Corice, J.R. Fox, K. Fox, The hypothetical chemical and spectroscopic activity of germane in the atmosphere of Jupiter, Icarus 16 (1972) 388–391, https://doi.org/10.1016/0019-1035(72)90082-6.

[4] U. Fink, H.P. Larson, R.R. Treffers, Germane in the atmosphere of Jupiter, Icarus 34 (1978) 344–354, https://doi.org/10.1016/0019-1035(78)90172-0.

[5] V. Kunde, R. Hanel, W. Maguire, D. Gautier, J.-P. Baluteau, A. Marten, A. Chédin, N. Husson, N. Scott, The tropospheric gas composition of the North Equatorial Belt (NH_3, PH_3, CH_3D, GeH_4, H_2O) and the Jovian D/H isotopic ratio, Astrophys. J. 263 (1982) 443–467, https://ntrs.nasa.gov/api/citations/19820012229/downloads/19820012229.pdf.

[6] P. Drossart, T. Encrenaz, V. Kunde, R. Hanel, M. Combes, An estimate of the PH_3, NH_3, CH_3D and GeH_4 abundances on Jupiter from the Voyager IRIS data at 4.5 μm, Icarus 49 (1982) 416–426, https://doi.org/10.1016/0019-1035(82)90046-X.

[7] F. Chen, D.L. Judge, C.Y.R. Wu, J. Caldwell, H.P. White, R. Wagener, High-resolution, low–temperature photoabsorption cross sections of C_2H_2, PH_3, AsH_3, and GeH_4, with application to Saturn's atmosphere, J. Geophys. Res. 96 (1991) 17519–17527, https://doi.org/10.1029/91JE01687.

[8] S.K. Atreya, P.R. Mahaffy, H.B. Niemann, M.H. Wong, T.C. Owen, Composition and origin of the atmosphere of Jupiter – an update, and implications for the extrasolar giant planets, Planetary space science 51 (2003) 105–112, https://doi.org/10.1016/S0032-0633(02)00144-7.

[9] K. Lodders, Jupiter formed with more tar than ice, Astrophys. J. 611 (2004) 587–597, http://iopscience.iop.org/0004-637X/.

[10] M. Asplund, N. Grevesse, J. Sauval, P. Scott, The chemical composition of the Sun, Ann. Rev. Astron. Astrophys. 47 (2009) 451–522, https://doi.org/10.1146/annurev.astro.46.060407.145222.

[11] K. Lodders, Atmospheric chemistry of the gas giant planets. Geochemical Society, 2010. https://www.geochemsoc.org/publications/geochemicalnews/gn142jan10/atmosphericchemistryoftheg/.

[12] M. Quack, Concept of Law in Chemistry: The concept of law and models in chemistry, European Rev. 22 (2014) S50–S86, https://doi.org/10.1017/S106279871300077X.

[13] H. Schwarz, Chemistry with methane: Concepts rather than recipes, Angewandte Chem. 50 (2011) 10096–10115, https://doi.org/10.1002/anie.201006424.

[14] G. Thyagarajan, J. Herranz, F.F. Cleveland, Potenial energy constants and rotational distortion constants for SiH_4, SiD_4, GeH_4, and GeD_4, J. Mol. Spectrosc. 7 (1961) 154–158, https://doi.org/10.1016/0022-2852(61)90349-6.

[15] A.V. Nikitin, M. Rey, A. Rodina, B.M. Krishna, V.G. Tyuterev, Full–dimensional potential energy and dipole moment surfaces of GeH_4 molecule and accurate first–principle rotationally resolved intensity predictions in the infrared, J. Phys. Chem. A 45 (2016) 8983–8997, https://doi.org/10.1021/acs.jpca.6b07732.

[16] H.W. Kattenberg, W. Gabes, A. Oskam, Infrared and laser Raman gas spectra of GeH_4, J. Mol. Spectrosc. 44 (1972) 425–442, https://doi.org/10.1016/0022-2852(72)90255-X.

[17] I.O. Ozier, A. Rosenberg, The forbidden rotational spectrum of GeH_4 in the Ground Vibronic State, Can. J. Phys. 51 (1973) 1882–1895, https://doi.org/10.1139/p73-249.

[18] R.F. Curl Jr, T. Oka, D.S. Smith, The observation of a pure rotational Q–branch transition of methane by infrared–radio frequency double resonance, J Mol Spectrosc 46 (1973) 518–520, https://doi.org/10.1016/0022-2852(73)90066-0.

[19] R.F. Curl Jr, Infrared-radio frequency double resonance observations of pure rotational Q-branch transitions of methane, J. Mol. Spectrosc. 48 (1973) 165–173, https://doi.org/10.1016/0022-2852(73)90145-8.

[20] W.A. Kreiner, T. Oka, Infrared – radio-frequency double resonance observations of $\Delta J = 0$ "forbidden" rotational transitions of SiH_4, Can. J. Phys. 53 (1975) 2000–2006, https://doi.org/10.1139/p75-250.

[21] R.H. Kagann, I. Ozier, M.C.L. Gerry, The centrifugal distortion dipole moment of silane, J. Chem. Phys. 64 (1976) 3487–3488, https://doi.org/10.1063/1.432605.

[22] P. Lepage, R. Brégier, R. Saint-Loup, La bande ν_3 du germane, C.R. Acad. Sci. Ser. B B 283 (1976) 179–180.

[23] W.A. Kreiner, U. Andresen, T. Oka, Infrared–microwave double resonance spectroscopy of GeH_4, J. Chem. Phys. 66 (1977) 4662–4665, https://doi.org/10.1063/1.433721.

[24] W.A. Kreiner, B.J. Orr, U. Andresen, T. Oka, Measurement of the centrifugal–distortion dipole moment of GeH_4 using a CO_2 laser, Phys. Rev. A 15 (1977) 2298–2304, https://doi.org/10.1103/PhysRevA.15.2298.

[25] S.J. Daunt, G.W. Halsey, K. Fox, R.J. Lovell, N.M. Gailar, High–resolution infrared spectra of ν_3 and $2\nu_3$ of germane, J. Chem. Phys. 68 (1978) 1319–1321, https://doi.org/10.1063/1.435861.

[26] R.J. Corice, Theoretical absolute J-manifold intensities of the ν_3 fundamental of GeH_4, J. Quant. Spectrosc. Radiat. Transf. 20 (1978) 65–69, https://doi.org/10.1016/0022-4073(78)90007-9.

[27] R.H. Kagann, I. Ozier, G.A. McRae, M.C.L. Gerry, The distortion moment spectrum of GeH_4: the microwave Q branch, Can. J. Phys. 57 (1979) 593–600, https://doi.org/10.1139/p79-083.

[28] K. Fox, G.W. Halsey, S.J. Daunt, R.C. Kennedy, Transition moment for ν_3 of $^{74}GeH_4$, J. Chem. Phys. 70 (1979) 5326–5327, https://doi.org/10.1063/1.437335.

[29] W.A. Kreiner, G. Magerl, B. Furch, E. Bonek, IR laser sideband observations in GeH_4 and CD_4, J. Chem. Phys. 70 (1979) 5016–5020, https://doi.org/10.1063/1.437342.

[30] G. Magerl, W. Schupita, E. Bonek, W.A. Kreiner, Observation of the isotope effect in the ν_2 fundamental of germane, J. Chem. Phys. 72 (1980) 395–398, https://doi.org/10.1063/1.438862.

[31] W.A. Kreiner, R. Opferkuch, A.G. Robiette, P.H. Turner, The ground–state rotational constants of Germane, J. Mol. Spectrosc. 85 (1981) 442–448, https://doi.org/10.1016/0022-2852(81)90215-0.

[32] P. Lepage, J.P. Champion, A.G. Robiette, Analysis of the ν_3 and ν_1 infrared bands of GeH_4, J. Mol. Spectrosc. 89 (1981) 440–448, https://doi.org/10.1016/0022-2852(81)90037-0.

[33] P.P. Das, V. Malathy Devi, A.G. Robiette, Tunable diode laser study of the ν_4 infrared band of GeH_4, J. Mol. Spectrosc. 91 (1982) 416–423, https://doi.org/10.1016/0022-2852(82)90159-X.

[34] J. Bunnell, T.A. Ford, Intramolecular coupling of vibrational modes and the assignments of the partially deuterated dihalogenomethanes, –silanes, and –germanes, J. Mol. Spectrosc. 100 (1983) 215–233, https://doi.org/10.1016/0022-2852(83)90083-8.

[35] A.E. Cheglokov, Yu.A. Kuritsin, E.P. Snegirev, O.N. Ulenikov, G.V. Vedeneeva, High–resolution spectroscopy of the ν_2 Q branch of GeH_4 with a computer–assisted, pulsed–diode laser spectrometer, J. Mol. Spectrosc. 105 (1984) 385–396, https://doi.org/10.1016/0022-2852(84)90228-5.

[36] R.D. Schaeffer, R.W. Lovejoy, Absolute line strengths of $^{74}GeH_4$ near 5 μ m, J. Mol. Spectrosc. 113 (1985) 310–314, https://doi.org/10.1016/0022-2852(85)90270-X.

[37] J. Cadot, Line strengths and pressure broadening by hydrogen in the spectrum of germane near 2110 cm^{-1}, J. Quant. Spectrosc. Radiat. Transf. 34 (1985) 331–334, https://doi.org/10.1016/0022-4073(85)90106-2.

[38] K. Ohno, H. Matsuura, Y. Endo, E. Hirota, The microwave spectra of deuterated silanes, germanes, and stannanes, J. Mol. Spectrosc. 118 (1986) 1–17, https://doi.org/10.1016/0022-2852(86)90219-5.

[39] P. Varanasi, S. Chudamani, Intensities and H_2-broadened half–widths of Germane lines around 4.7 μm at temperatures relevant to Jupiter's atmosphere, J. Quant. Spectrosc. Radiat. Transf. 38 (1987) 173–177, https://doi.org/10.1016/0022-4073(87)90081-1.

[40] Q.-S. Zhu, B.A. Thrush, A.G. Robiette, Local mode rotational structure in the (3000) Ge-H stretching overtone ("$3\nu_3$") of germane, Chem. Phys. Lett. 150 (1988) 181–183, https://doi.org/10.1016/0009-2614(88)80023-X.

[41] L. Halonen, Stretching vibrational states in Germane, J. Phys. Chem. 93 (1989) 631–634, https://doi.org/10.1021/j100339a027.

[42] Q. Zhu, B.A. Thrush, Rotational structure near the local mode limit in the (3000) band of germane, J. Chem. Phys. 92 (1990) 2691–2697, https://doi.org/10.1063/1.458582.

[43] Q. Zhu, H. Qian, B.A. Thrush, Rotational analysis of the (2000) and (3000) bands and vibration-rotation interaction in germane local mode states, Chem. Phys. Lett. 186 (1991) 436–440, https://doi.org/10.1016/0009-2614(91)90205-N.

[44] A. Campargue, J. Vetterhöffer, M. Chenevier, Rotationally resolved overtone transitions of $^{70}GeH_4$ in the visible and near-infrared, Chem. Phys. Lett. 192 (1992) 353–356, https://doi.org/10.1016/0009-2614(92)85481-O.

[45] Q. Zhu, A. Campargue, J. Vetterhöffer, D. Permogorov, F. Stoeckel, High resolution spectra of GeH_4 v = 6 and 7 stretch overtones. The perturbed local mode vibrational states, J. Chem. Phys. 99 (1993) 2359–2364, https://doi.org/10.1063/1.465251.

[46] J. Liao, Q.-S. Zhu, Interpretation of the relative intensities of the (4000), (3100), and (5000) local–mode vibrational bands of germane, J. Mol. Spectrosc. 183 (1997) 414–416, https://doi.org/10.1006/jmsp.1997.7264.

[47] F. Sun, X. Wang, J. Liao, Q. Zhu, The (5000) Local Mode Vibrational State of Germane: A high-resolution spectroscopic study, J. Mol. Spectrosc. 184 (1997) 12–21, https://doi.org/10.1006/jmsp.1997.7281.

[48] X.Y. Chen, H. Lin, X.G. Wang, K. Deng, Q.S. Zhu, High–resolution Fourier transform spectrum of the (4000) local mode overtone of GeH_4: local mode effect, J. Mol. Struct. 517–518 (2000) 41–51, https://doi.org/10.1016/S0022-2860(99)00237-9.

[49] G. Pierre, V. Boudon, E.B. MKadmi, H. Bürger, D. Bermejo, Martínez, Study of the fundamental bands of $^{70}GeD_4$ by high–resolution Raman and infrared spectroscopy: First experimental determination of the equilibrium bond length of germane, J. Mol. Spectrosc. 216 (2002) 408–418, https://doi.org/10.1006/jmsp.2002.8662.

[50] M. Litz, H. Bürger, A. Campargue, Observation by ICLAS VeCSEL technique, and rotational analysis, of the ΔGeH=5 stretching vibrational overtone of $H_3^{70}GeD$, J. Mol. Spectrosc. 226 (2004) 182–189, https://doi.org/10.1016/j.jms.2004.03.010.

[51] O.N. Ulenikov, O.V. Gromova, E.S. Bekhtereva, N.I. Raspopova, P.G. Sennikov, M.A. Koshelev, I.A. Velmuzhova, A.P. Velmuzhov, High resolution study of $^{M}GeH_4$ (M=76, 74) in the dyad region, J. Quant. Spectrosc. Radiat. Transf. 144 (2014) 11–26, https://doi.org/10.1016/j.jqsrt.2014.03.025.

[52] O.N. Ulenikov, O.V. Gromova, E.S. Bekhtereva, N.I. Raspopova, A.L. Fomchenko, P.G. Sennikov, M.A. Koshelev, I.A. Velmuzhova, A.P. Velmuzhov, First high resolution ro–vibrational study of the (0200), (0101) and (0002)

vibrational states of $^{M}GeH_4$ (M = 76,74), J. Quant. Spectrosc. Radiat. Transf. 182 (2016) 199–218, https://doi.org/10.1016/j.jqsrt.2016.05.014.
[53] O.N. Ulenikov, O.V. Gromova, E.S. Bekhtereva, N.I. Raspopova, P.G. Sennikov, M.A. Koshelev, I.A. Velmuzhova, A.P. Velmuzhov, S.A. Adamchik, High resolution study of strongly interacting $2\nu_1(A_1)/\nu_1+\nu_3(F_2)$ bands of $^{M}GeH_4$ (M = 76, 74), J. Quant. Spectrosc. Radiat. Transf. 205 (2018) 96–107, https://doi.org/10.1016/j.jqsrt.2017.09.025.
w[54] O.N. Ulenikov, O.V. Gromova, E.S. Bekhtereva, N.I. Raspopova, M.A. Koshelev, I.A. Velmuzhova, A.D. Bulanov, P.G. Sennikov, High–resolution FTIR spectroscopic study of $^{73}GeH_4$ up to 2300 cm^{-1}, J. Quant. Spectrosc. Radiat. Transf. 221 (2018) 129–137, https://doi.org/10.1016/j.jqsrt.2018.09.023.
[55] V. Boudon, T. Grigoryan, F. Philipot, C. Richard, F. Kwabia Tchana, L. Manceron, et al., Line positions and intensities for the ν_3 band of 5 isotopologues of germane for planetary applications, J. Quant. Spectrosc. Radiat. Transf. 205 (2018) 174–183, https://doi.org/10.1016/j.jqsrt.2017.10.017.
[56] O.N. Ulenikov, O.V. Gromova, E.S. Bekhtereva, N.I. Raspopova, A.V. Kuznetsov, M.A. Koshelev, I.A. Velmuzhova, P.G. Sennikov, First high–resolution comprehensive analysis of $^{72}GeH_4$ spectra in the Dyad and Pentad regions, J. Quant. Spectrosc. Radiat. Transf. 225 (2019) 206–213, https://doi.org/10.1016/j.jqsrt.2018.12.036.
[57] O.N. Ulenikov, O.V. Gromova, E.S. Bekhtereva, N.I. Raspopova, A.V. Kuznetsov, C. Sydow, S. Bauerecker, High resolution analysis of GeH_4 in the dyad region: Ro–vibration energy structure of $^{70}GeH_4$ and line strengths of $^{M}GeH_4$ (M = 70, 72, 73, 74, 76), J. Quant. Spectrosc. Radiat. Transf. 236 (2019) 106581, https://doi.org/10.1016/j.jqsrt.2019.106581.
[58] O.N. Ulenikov, O.V. Gromova, E.S. Bekhtereva, N.I. Raspopova, M.A. Koshelev, I.A. Velmuzhova, P.G. Sennikov, A.D. Bulanov, A.V. Kuznetsov, C. Leroy, First high–resolution analysis of the $2\nu_1(A_1)$ and $\nu_1+\nu_3(F_2)$ interacting states of $^{72}GeH_4$ and $^{73}GeH_4$, J. Quant. Spectrosc. Radiat. Transf. 236 (2019) 106593, https://doi.org/10.1016/j.jqsrt.2019.106593.
[59] O.N. Ulenikov, O.V. Gromova, E.S. Bekhtereva, N.I. Raspopova, K. Berezkin, C. Sydow, S. Bauerecker, Line strengths analysis of germane in the 1100–1350 cm^{-1} region: the ν_1-ν_4, ν_3-ν_4, ν_3-ν_2 and ν_1-ν_2 "hot" bands of $^{M}GeH_4$ (M = 70, 72, 73, 74, 76), J. Quant. Spectrosc. Radiat. Transf. 242 (2020) 106755, https://doi.org/10.1016/j.jqsrt.2019.106755.
[60] C. Richard, V. Boudon, M. Rotger, Calculated spectroscopic databases for the VAMDC portal: New molecules and improvements, J. Quant. Spectrosc. Radiat. Transfer. 251 (2020) 107096, https://doi.org/10.1016/j.jqsrt.2020.107096.
[61] O.N. Ulenikov, O.V. Gromova, E.S. Bekhtereva, N.I. Raspopova, A.V. Kuznetsov, V. Boudon, C. Sydow, K. Berezkin, S. Bauerecker, Comprehensive study of the pentad bending triad region of germane: Positions, strengths, widths and shifts of lines in the $2\nu_2$, $\nu_2+\nu_4$, and $2\nu_4$ bands of $^{70}GeH_4$, $^{72}GeH_4$, $^{73}GeH_4$, $^{74}GeH_4$, $^{76}GeH_4$, J. Quant. Spectrosc. Radiat. Transf. 242 (2020) 106755, https://doi.org/10.1016/j.jqsrt.2021.107526.
[62] C. Richard, V. Boudon, A. Rizopoulos, J. Vander Auwera, F. Kwabia Tchana, Line positions and intensities for the ν_2/ν_4 bands of 5 isotopologues of germane near 11.5 μm, J. Quant. Spectrosc. Radiat. Transf. 260 (2021) 107474, https://doi.org/10.1016/j.jqsrt.2020.107474.
[63] J.-P. Champion, J.-C. Hilico, C. Wenger, Analysis of the ν_2/nu_4 dyad of $^{12}CH_4$ and $^{13}CH_4$, J. Mol. Spectrosc. 133 (1989) 256–272, https://doi.org/10.1016/0022-2852(89)90193-8.
[64] J.-C. Hilico, O. Robert, M. Loëte, S. Toumi, A.S. Pine, L.R. Brown, Analysis of the interacting octad system of $^{12}CH_4$, J. Mol. Spectrosc. 208 (2001) 1–13, https://doi.org/10.1006/jmsp.2001.8364.
[65] J.-J. Zheng, O.N. Ulenikov, G.A. Onopenko, E.S. Bekhtereva, S.-G. He, X.-H. Wang, S.-M. Hu, H. Lin, Q.-S. Zhu, High resolution vibration–rotation spectrum of the D2O molecule in the region near the $2\nu_1+\nu_2+\nu_3$ absorption band, Mol. Phys. 99 (2001) 931–937, https://doi.org/10.1080/00268970010028854.
[66] O.N. Ulenikov, E.S. Bekhtereva, Y. Krivchikova, Y. Morzhikova, T. Buttersack, C. Sydow, S. Bauerecker, High resolution analysis of $^{32}S^{18}O_2$ spectra: The ν_1 and ν_3 interacting bands, J. Quant. Spectrosc. Radiat. Transf. 166 (2015) 13–22, https://doi.org/10.1016/j.jqsrt.2015.07.004.
[67] O.N. Ulenikov, H. Bürger, W. Jerzembeck, G.A. Onopenko, E.S. Bekhtereva, O.L. Petrunina, The ground vibrational states of PH_2D and PHD_2, J. Mol. Struct. 599 (2001) 225–237, https://doi.org/10.1016/S0022-2860(01)00826-2.
[68] O.N. Ulenikov, G.A. Ushakova, Analysis of the H_2O molecule second–hexade interacting vibrational states, J. Mol. Spectrosc. 117 (1986) 195–205, https://doi.org/10.1016/0022-2852(86)90149-9.
[69] O.N. Ulenikov, R.N. Tolchenov, Q.-S. Zhu, "Expanded" local mode approach for $XY_2(C_{2v})$ molecules, Spectrochim. Acta 52 (1996) 1829–1841, https://doi.org/10.1016/S0584-8539(96)01749-7.
[70] O.N. Ulenikov, O.V. Gromova, E.S. Bekhtereva, A.L. Fomchenko, C. Sydow, S. Bauerecker, First high resolution analysis of the $3\nu_1$ band of $^{34}S^{16}O_2$, J. Mol. Spectrosc. 319 (2016) 50–54, https://doi.org/10.1016/j.jms.2015.11.002.
[71] S.-M. Hu, O.N. Ulenikov, G.A. Onopenko, E.S. Bekhtereva, S.-G. He, X.-H. Wang, H. Lin, Q.-S Zhu, High–resolution study of strongly interacting vibrational bands of HDO in the region 7600-8100 cm^{-1}, J. Mol. Spectrosc. 203 (2000) 228–234, https://doi.org/10.1006/jmsp.2000.8173.
[72] S.A. Adamchik, A.D. Bulanov, P.G. Sennikov, M.F. Churbanov, A.Yu. Sozin, O.Yu. Chernova, I.A. Kosheleva, O.Yu. Troshin, Ultrapurification of ^{76}Ge–enriched GeH_4 by distillation, Inorg. Mater. 47 (2011) 694–696, https://doi.org/10.1134/S0020168511070016.
[73] I.E. Gordon, L.S. Rothman, C. Hill, R.V. Kochanov, Y. Tan, P.F. Bernath, et al., The HITRAN 2016 molecular spectroscopic database, J. Quant. Spectrosc. Radtat. Transf. 203 (2017) (2016) 3–69, https://doi.org/10.1016/j.jqsrt.2017.06.038.
[74] K.T. Hecht, The vibration–rotation energies of tetrahedral XY_4 molecules: Part I. Theory of spherical top molecules, J. Mol. Spectrosc. 5 (1960) 355–389, https://doi.org/10.1016/0022-2852(61)90102-3.
[75] H.M. Niederer, The infrared spectrum of methane, Verlag Dr. Hut, Munchen, 2012.
[76] H.M. Niederer, X.G. Wang, T. Carrington, S. Albert, S. Bauerecker, V. Boudon, M. Quack, Analysis of the rovibrational spectrum of $^{13}CH_4$ in the octad range, J. Mol. Spectrosc. 291 (2013) 33–47, https://doi.org/10.1016/j.jms.2013.06.003.
[77] O.N. Ulenikov, O.V. Gromova, E.S. Bekhtereva, N.I. Raspopova, I.A. Velmuzhova, M.A. Koshelev, P.G. Sennikov, First high-resolution analysis of the $3\nu_4$, $\nu_2+2\nu_4$ and $2\nu_2+\nu_4$ bands of $^{76}GeH_4$, J. Quant. Spectrosc. Radiat. Transf. 262 (2021) 107517, https://doi.org/10.1016/j.jqsrt.2021.107517.
[78] U. Fano, G. Racah, Irreducible tensorial sets, Academic Press, NewYork, 1959.
[79] E.P. Wigner, Quantum theory of angular momentum, Academic Press, NewYork, 1965.
[80] D.A. Varshalovitch, A.N. Moskalev, V.K. Khersonsky, Quantum theory of angular momentum, Nauka, Leningrad, 1975.
[81] V. Boudon, J.P. Champion, T. Gabard, M. Loëte, M. Rotger, C. Wenger, Spherical top theory and molecular spectra, in: M. Quack, F. Merkt (Eds.), Handbook of high–resolution spectroscopy, vol. 3, Wiley, 2011, pp. 1437–1460. https://doi.org/10.1002/9780470749593.hrs021.
[82] J. Moret-Bailly, Sur l'interprétation des spectres de vibration–rotation des molécules à symétrie tétraédrique ou octaédrique, Cah. Phys. 15 (1961) 237–314.
[83] J.P. Champion, G. Pierre, F. Michelot, J. Moret-Bailly, Composantes cubiques normales des tenseurs spheriques, Can. J. Phy.s 55 (1977) 512–520, https://doi.org/10.1139/p77-070.
[84] J.P. Champion, Developpement complet de l'hamiltonien de vibration–rotation adapté à l'etude des interactions dans les molécules toupies sphériques. Application aux bandes ν_2 et ν_4 de $^{12}CH_4$, Can. J. Phys. 55 (1977) 1802–1828, https://doi.org/10.1139/p77-221.
[85] V. Boudon, J.P. Champion, T. Gabard, M. Loëte, F. Michelot, G. Pierre, M. Rotger, C. Wenger, M. Rey, Symmetry–adapted tensorial formalism to model rovibrational and rovibronic spectra of molecules pertaining to various point groups, J. Mol. Spectrosc. 228 (2004) 620–634, https://doi.org/10.1016/j.jms.2004.02.022.
[86] A.E. Cheglokov, O.N. Ulenikov, A.S. Zhilyakov, V.N. Cherepanov, Yu.S. Makushkin, A.B. Malikova, On the determination of spectroscopic constants as functions of intramolecular parameters, J. Phys. B 22 (1989) 997–1015, https://doi.org/10.1088/0953-4075/22/7/009.
[87] H.H. Nielsen, The vibration–rotation energies of molecules, Rev. Mod. Phys. 23 (1951) 90–136, https://doi.org/10.1103/RevModPhys.23.90.
[88] J.K.G. Watson, Determination of centrifugal distortion coefficients of asymmetric–top molecules, J. Chem. Phys. 46 (1967) 1935–1949, https://doi.org/10.1063/1.1840957.
[89] D. Papousek, M.R. Aliev, Molecular vibrational–rotational spectra, Elsevier, Amsterdam, 1982.
[90] O.N. Ulenikov, S.-G. He, G.A. Onopenko, E.S. Bekhtereva, X.-H. Wang, S.-M. Hu, H. Lin, Q.-S. Zhu, High-Resolution Study of the $(\nu_1 + 1/2\nu_2 + \nu_3 = 3)$ Polyad of Strongly Interacting Vibrational Bands of D_2O, J. Mol. Spectrosc. 204 (2000) 216–225, https://doi.org/10.1006/jmsp.2000.8221.
[91] A.D. Bykov, Yu.S. Makushkin, O.N. Ulenikov, The vibrational analysis of $H_2^{16}O$, J. Mol. Spectrosc. 99 (1983) 221–227, https://doi.org/10.1016/0022-2852(83)90305-3.
[92] O.N. Ulenikov, S.-M. Hu, E.S. Bekhtereva, G.A. Onopenko, S.-G. He, X.-H. Wang, J.-J. Zheng, Q.-Z. Zhu, High-resolution Fourier transform spectrum of D_2O in the region near 0.97 μm, J. Mol. Spectrosc. 210 (2001) 18–27, https://doi.org/10.1006/jmsp.2001.8433.
[93] O.N. Ulenikov, O.V. Gromova, E.S. Bekhtereva, I.B. Bolotova, I.A. Konov, V.-M. Horneman, C. Leroy, High resolution analysis of the SO_2 spectrum in the 2600–2900 cm^{-1} region: $2\nu_3$, $\nu_2+2\nu_3$-ν_2 and $2\nu_1+\nu_2$ bands, J. Quant. Spectrosc. Radiat. Transf. 113 (2012) 500–517, https://doi.org/10.1016/j.jqsrt.2012.01.006.
[94] B.I. Zhilinskii, Method of irreducible tensorial sets in molecular spectroscopy (in Russian), Moscow State University Press, Moscow, 1981.
[95] J. Moret-Bailly, L. Gautier, J. Montagutelli, Clebsch-Gordan coefficients adapted to cubic symmetry, J. Mol. Spectrosc. 15 (1965) 355–377, https://doi.org/10.1016/0022-2852(65)90151-7.
[96] M. Rey, V. Boudon, Ch. Wenger, G. Pierre, B. Sartakhov, Orientation of O(3) and $SU(2)\otimes C_I$ representation in cubic point groups (O_h, T_d) for application to molecular spectroscopy, J. Mol. Spectrosc. 219 (2003) 313–325, https://doi.org/10.1016/S0022-2852(03)00056-0.
[97] M. Loëte, Développement complet du moment dipolaire des molécules tétraédriques. Application aux bandes triplement dégénérées et à la diade ν_2 et ν_4, Can. J. Phys. 61 (1983) 1242–1259, https://doi.org/10.1139/p83-158.
[98] C. Wenger, V. Boudon, J.P. Champion, G. Pierre, Highly–spherical top data system (HTDS) software for spectrum simulation of octahedral XY-6 molecules, J. Quant. Spectrosc. Radiat. Transf. 66 (2000) 1–16, https://doi.org/10.1016/S0022-4073(99)00161-2.
[99] M.A. Koshelev, A.P. Velmuzhov, I.A. Velmuzhova, P.G. Sennikov, N.I. Raspopova, E.S. Bekhtereva, O.V. Gromova, O.N. Ulenikov, High resolution

study of strongly interacting $\nu_1(A_1)/\nu_3(F_2)$ bands of ^{M}GeH4 (M = 76, 74), J. Quant. Spectrosc. Radiat. Transf. 164 (2015) 161–174, https://doi.org/10.1016/j.jqsrt.2015.06.003.

[100] S. Albert, S. Bauerecker, V. Boudon, L.R. Brown, J.-P. Champion, M. Loete, A. Nikitin, M. Quack, Global analysis of the high resolution infrared spectrum of methane $^{12}CH_4$ in the region from 0 to 4800 cm^{-1}, Chem. Phys. 356 (2009) 131–146, https://doi.org/10.1016/j.chemphys.2008.10.019.

[101] M. Terki-Hassaïne, Ch. Claveau, A. Valentin, G. Pierre, Analysis of the infrared Fourier transform spectrum of the spectra of Silane in the range 2930–3300 cm^{-1}, J. Mol. Spectrosc. 197 (1999) 307–321, https://doi.org/10.1006/jmsp.1999.7921.

[102] A.D. Bykov, Yu.S. Makushkin, O.N. Ulenikov, On isotope effects in polyatomic molecules. Some comments on the method, J. Mol. Spectrosc. 85 (1981) 462–479, https://doi.org/10.1016/0022-2852(81)90217-4.

[103] A.D. Bykov, Yu.S. Makushkin, O.N. Ulenikov, On the displacements of centers of vibration-rotation bands under isotope substitution in polyatomic molecules, J. Mol. Spectrosc. 93 (1982) 46–54, https://doi.org/10.1016/0022-2852(82)90273-9.

[104] A.D. Bykov, Yu.S. Makushkin, O.N. Ulenikov, On the displacements of centres of vibration-rotation lines under isotope substitution in polyatomic molecules, Mol. Phys. 51 (1984) 907–918, https://doi.org/10.1080/00268978400100601.